

# THE ZEUS HADRON ELECTRON SEPARATOR, PERFORMANCE AND EXPERIENCE

P. GÖTTLICHER

*Deutsches Elektronen-Synchrotron DESY, Hamburg, Germany  
E-mail: Peter.Goettlicher@desy.de*

*(For the ZEUS-HES Group)*

The hadron electron separator (HES), a component of the ZEUS experiment is designed to improve the identification of electrons generally and, in particular, within jets. It consists of 20518 silicon diodes with  $20m^2$  active area. The diodes are installed after 3–5  $X_0$  of the electromagnetic uranium-calorimeter, where the maximum intensity of the shower is expected. With an analog readout of each channel the deposited energy is measured. The HES improves the electron identification by a energy dependent factor 2.5 to 5 and the granularity by a factor 10. The attained position resolution is  $5.4mm$ .

## 1. Introduction

In HERA at DESY protons ( $820GeV/920GeV$ ) collide with  $27.5GeV$  electrons or positrons. The scattered or produced  $e^\pm$  and  $\gamma$ 's have energies from very low values to a few  $100GeV$ . For example in DIS and heavy flavor physics it is important to study electrons with a few GeV. These electrons are identified with the tracking detectors and the calorimeter. A cross-section of the ZEUS detector is shown in figure 1<sup>1</sup>. The Uranium calorimeter contains forward (FCAL), barrel (BCAL) and rear (RCAL) elements which are longitudinally segmented into one electromagnetic and two hadronic sections readout separately as towers. Hadronic towers have  $20 \times 20cm^2$  and electromagnetic towers  $5 \times 20cm^2$  (FCAL,BCAL) and  $10 \times 20cm^2$  (RCAL) planar sizes. This is much broader than the radius of the electromagnetic shower  $R_{Molière} = 2cm$ . The measurement of the showers is improved by a highly segmented planar detector at a depth close to the shower maximum. This component called hadron electron separator (HES) consists of two circular planes of diodes, RHES and FHES, in the RCAL and FCAL with a radius of  $1.9m$ .

The HES uses the different showering behavior to distinguish  $e^\pm$  and  $\gamma$ 's from hadrons. Typically electromagnetic showers develop early into narrow cones while most hadronic particle showers start only deep inside the calorime-

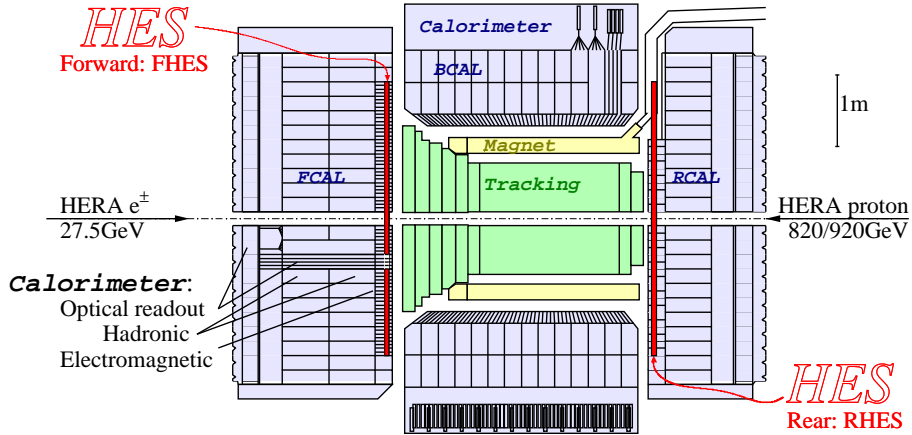


Figure 1. A cut through the inner part of the ZEUS detector along the beam line showing the tracking detector, the magnet and the calorimeter split into forward (FCAL), barrel (BCAL) and rear part (RCAL). The HES is the cross-hatched bar from the top to the bottom of the electromagnetic RCAL and FCAL.

ter. This leads to the idea of measuring the number of particles crossing a plane in the early stage of a shower. The position of the plane is chosen as  $3$  to  $5X_0$ , where the maximum intensity of the electromagnetic shower is expected. Comparing this position to the  $25X_0$  or  $1\lambda$  (nuclear interaction length) longitudinal

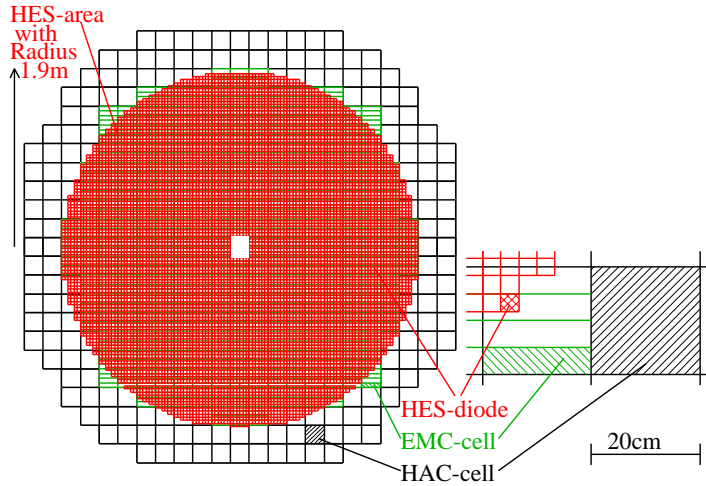


Figure 2. A view of the front face of the FCAL together with a blow up where the cell sizes of the electromagnetic and hadronic calorimeter (EMC, HAC) and the HES are indicated.

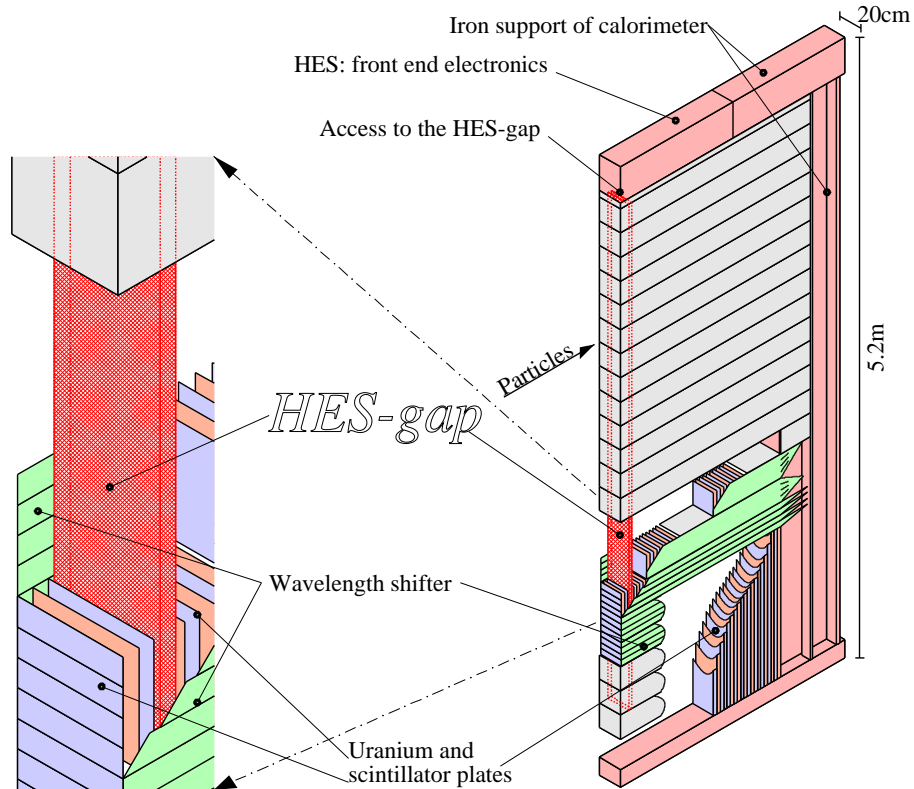


Figure 3. A module of the ZEUS forward calorimeter with the Uranium and scintillator plates, the optical readout and the HES.

segmentation of the calorimeter allows HES to identify electromagnetic showers more easily. The finer segmentation of the HES diodes,  $10\text{cm}^2$  in comparison with the  $5 \times 20\text{cm}^2$  or  $10 \times 20\text{cm}^2$  of the FCAL and RCAL, allows the HES to search for electromagnetic showers within jets.

## 2. Constraints on the design and the construction of the HES

How the HES is embedded into the calorimeter is sketched in figure 3<sup>1</sup>. The calorimeter consists of Uranium plates with a height of  $4.6\text{m}$ . These alternate with the scintillator plates. On the sides of the module wavelength shifters and light guides are mounted.

The HES is constructed to have a low impact on the energy measurement. Therefore the  $5\text{m}$  long gap after the fourth scintillator plate has a depth of only  $1.5\text{cm}$ . In the gap only a small amount of material has been installed, because

this is passive for the energy measurement and the position close to the shower maximum is most sensitive.

The Uranium, scintillator and wavelength shifters surround the gap in the horizontal plane completely and constrain the geometry. The only access to the gap is at the top of the calorimeter through an opening of  $16.3 \times 1.5 \text{cm}^2$ . Through this HES modules, with lengths equal to the  $4.6 \text{m}$  height of the active calorimeter, has to be installed including the infrastructure for 672 readout channels – cooling, power and signal lines.

As the gap is close to the tracking chambers the magnetic field of the solenoid at the HES-gap is close to the nominal  $1.4 \text{T}$ . The frontend electronics is housed in cabinets of the iron support structure on top of the calorimeter.

### 3. Experimental Setup

Silicon diodes forming the active medium have the advantage of producing a high electrical signal in a small volume and of being insensitive to the magnetic field. In the  $400 \mu\text{m}$  thick silicon minimum ionizing particles (MIP) produce 33000 electron-hole pairs. A compromise between number of channels and shower size  $R_{\text{Molière}}=2 \text{cm}$  leads to a size  $3.47 \times 3.07 \text{cm}^2$  of a diode with  $3.32 \times 2.96 \text{cm}^2$  being the active area<sup>2</sup>. This improves the granularity by a factor 10 compared to the cell size of the FCAL. Figure 4a illustrates, how 2 diodes and their preamplifiers are combined on one ceramic plate. The HES detector contains  $20 \text{m}^2$  of silicon or 20518 channels.

Since the available space is small and additional material worsens the energy resolution, central parts of the construction have multiple functionality. The multilayer board is used as a cable for 112 signals from 56 ceramic plates, supply and calibration lines. It also gives the HES-module the mechanical strength.

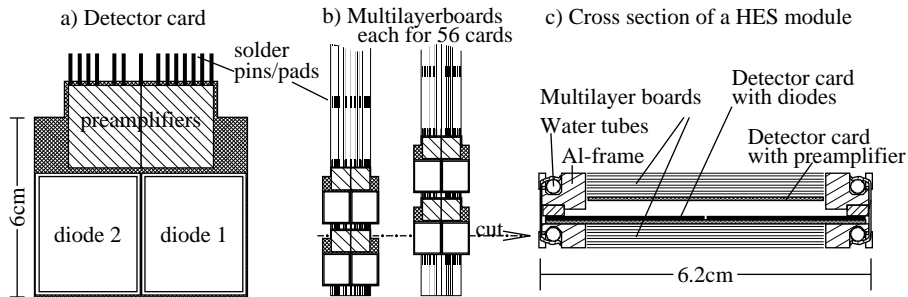


Figure 4. Construction of a HES module: a) a ceramic plate with 2 diodes and preamplifiers; b) equipment of 2 long multilayer boards. The full structure has 56 cards per multilayer board and a total length with connectors of  $4.6 \text{m}$  c) cross section through a closed module.

Since the signals have to be transported from the bottom of the CAL to the electronics on the top, these 18-layer boards have an unusual length of  $4.6m$ . Because of the special production techniques for such a length, no electrical connections between the layers are possible. The inner layers are contacted by cutouts in the layers above at the solder pads for the detector plates. Adverse effects on electrical signals is limited by keeping the capacitance of the signal lines below  $1nF$ . Nevertheless the rise time of the signal grows over the full length from  $50ns$  to  $100ns$ , which is compatible to the bunch crossing time of HERA.

Each multilayer board is equipped with up to 56 ceramic plates (figure 4b). Along the multilayer board the active areas of the diodes alternate with the preamplifiers and only half of the area is sensitive to particles. To get full coverage two of these structures are shifted against each another by the length of a diode and then folded over each another as depicted in figure 4c. Each diode faces a preamplifier of the opposite multilayer board. Together with a few additional mechanical parts a HES-module is formed containing two multilayer boards and 224 diodes. The robust parts covers the more sensitive diodes and electronics.

The power consumption of  $90mW/channel$  has to be water cooled, because the heat conductivity of the surrounding sandwich calorimeter is low and the gap is  $4.6m$  long.

Three modules with each 224 diodes are installed into each calorimeter module and covers, sitting side by side, the area between the wavelength shifters of the calorimeter with 672 diodes. HES adds  $0.1X_0$  of material to the calorimeter.

The active area of the HES diodes covers 94% of the area incident to particles. The non-sensitive area breaks down as follows: the field stop in the diodes before their mechanical edge: 2.5%, the mechanical construction of the modules: 2.5% and the limited size of the diodes: 0.5%, because of economical reasons four diodes are produced from a single 4-inch-wafer. In addition the wavelength shifters of the calorimeter pass the HES plane making 9.5% of the area inaccessible.

Figure 5 shows an overview of the further readout electronics. Inside the cabinets of the iron structure shaping amplifiers slow the rise time of the pulses to 180ns, which has the advantage of removing the position dependent effects within the multilayer board. The overlay of consecutive bunch crossings can be tolerated, since the interaction rate at HERA is much lower then the bunch crossing rate. With an integrated circuit<sup>3</sup> developed for the ZEUS-calorimeter the signal height is sampled each 96ns and stored in capacitors of a circular analog pipeline. This is overwritten until the ZEUS trigger decides to keep the

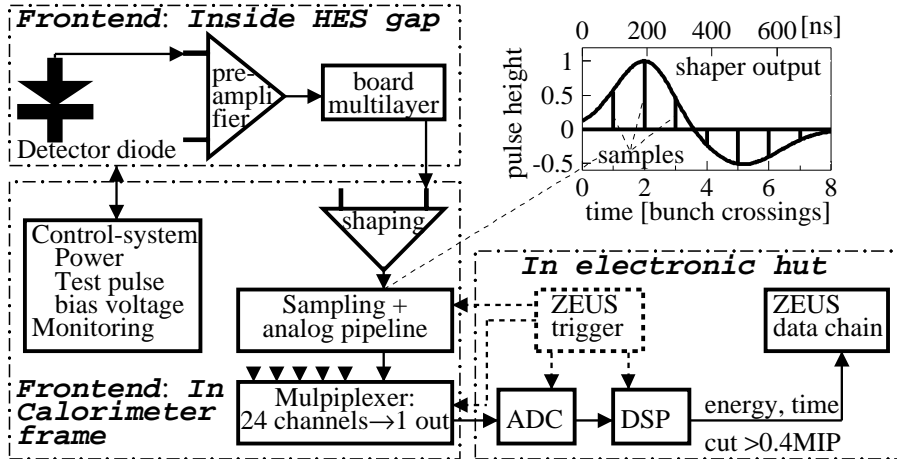


Figure 5. The electronic chain of the HES

data. Then 24 channels and four samples for each channel around the triggered bunch crossing are multiplexed to a single signal line. This reduces the multiplicity of cables to the electronic hut. After digitizing a DSP calculates the energy and the time of the diode signal and suppresses signals below 0.4MIP. Typically per trigger data from 5% of the channels are sent out to the ZEUS data acquisition chain.

#### 4. Performance and Experience

The calibration of the HES is performed by charge injection into the preamplifiers. Since drifts are very small this essentially identifies faults. The energy scale is checked with muons. At HERA halo- $\mu$  are produced far upstream of the ZEUS experiment and propagate parallel to the proton beam crossing the HES-plane perpendicularly. The energy deposition spectrum (figure 6) follows a peak fitted by a convolution of a Landau-distribution for the ionization with a Gaussian for the detector resolution<sup>4</sup>. The energy deposition of a MIP is  $120keV$ .

For electrons the energy of the shower is distributed to a few diodes. A typical cluster is shown in figure 7. The clustering algorithm used looks for a diode with a local maximum of energy deposition and associates all 8 neighbors to it. This algorithm is verified by analysing, how much more energy is measured in an enlarged area of  $5 \times 5$  diodes<sup>5</sup>. On average the cluster contains 96% of the energy, which is sufficient for electron identification. The incident position of the  $e^\pm$  and  $\gamma$ 's can be reconstructed by a weighted mean of the diode posi-

tions. The weighting coefficients are functions of the pulse heights. Away from the edges (85% of the HES area) the position resolution is measured with test beams to be  $5.4\text{mm}$  for  $25\text{GeV}$   $e^\pm$  (figure 7)<sup>6</sup>. The Monto-Carlo simulation describes the data for DIS electrons ( $\approx 25\text{GeV}$ ) well and shows a resolution of  $5\text{mm}$  inside the ZEUS experiment<sup>7</sup>.

The improvement for the electron/hadron separation was measured with clean samples at test beams. Hadrons and electrons show distinguishable spectrums with a relatively low misidentification probability (figure 6)<sup>1</sup>. A cut with 90% electron identification efficiency has been defined. In table 1 the misidentification rates for calorimeter only, HES only and combined measurements are shown. For the calorimeter data the analysis is restricted to a tower with a front surface of  $20 \times 20\text{cm}^2$ , to adapt the analysis to the real situation at ZEUS with jets. Using HES improves the misidentification by a factor between 2.5 and 5 depending on energy.

The HES was installed into the ZEUS experiment as a second stage upgrade. The plane in the rear calorimeter (RHES) was installed during the years 1992 to 1994 and the plane in the front calorimeter (FHES) from 1996 to 1998. FHES was operated since then until 2000 with a bad channel rate of 2 to 3% and RHES until 1999 with a bad channel rate of 3 to 6%. The reason for these

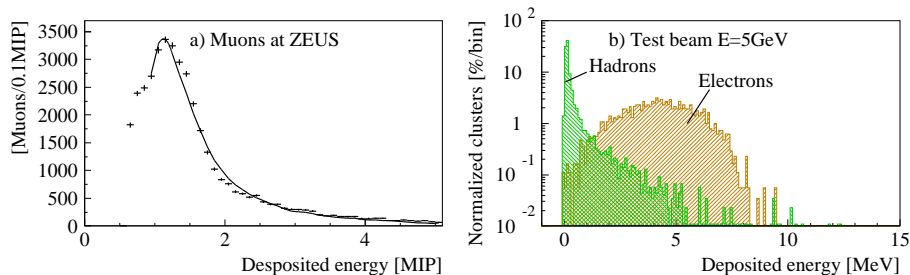


Figure 6. Energy deposition in the HES a) Muons b) 5GeV electrons and hadrons

Table 1. Rate of misidentified hadrons in [%] for 90%  $e^-$  efficiency.

Used detector	Energy			
	2 GeV	3 GeV	5 GeV	9 GeV
Calorimeter	7.79%	4.03%	0.65%	0.37%
HES	3.8%	3.4%	3.5%	3.6%
HES and calorimeter combined	1.47%	0.86%	0.22%	0.15%
Factor of improvement by HES	5.3	4.7	3.0	2.5

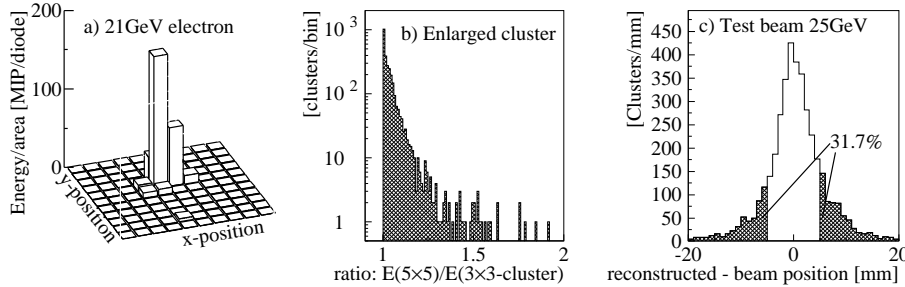


Figure 7. Cluster for electrons: a) a typical cluster for a 21 GeV  $e^-$ , each tower corresponds to a diode; b) spectrum of the energy ratio in an increased area ( $5 \times 5$  diodes) to the  $3 \times 3$ -cluster; c) Position resolution for 25 GeV  $e^-$  away from the edges of the HES area.

failure rate are mainly connectors. To keep this rate low continuous repairs on detector access days are made. The number of broken and repaired channels of 100/month is mainly due to the fact, that a single faults effects large groups of channels. In the RHES water leakages developed during the year 1999. The copper tubes used inside the HES-gap of the calorimeter has a wall thickness of only 0.3mm to keep space and material low (figure 4). These tubes corroded from the inside. Later water analysis showed traces of sulfate-ions and organic molecules, both are known to speed up corrosion. The extensive repairs were possible during the long shutdown for the HERA luminosity upgrade and the complete HES is prepared for the HERA-II runs.

### Acknowledgements

The HES is an international project. I thank all contributors – physicists, engineers and technicians – from Germany, Israel, Japan, Korea , Russia, Spain and the USA for their combined effort.

### References

1. The ZEUS-Detector, Status-Report 1993, ed. U.Holm, DESY 1993
2. K.H. Barth, Messungen zur Homogenitaet des ZEUS Hadron-Elektron-Separators, Diploma-Thesis, University Hamburg (1991)
3. W. Buttler et al., Design and Performance of a 10MHz CMOS Analog Pipeline, *Nucl. Instr. Meth.* **A277**, 217 (1989)
4. T.Kuhn-Sander, Untersuchung von Strahl-Halo Myonen im ZEUS Detektor, Internal Note DESY F35D-96-15, DESY (1996)
5. J.I. Fleck, K. Ohrenberg, Electron Identification in the HES and a new way to determine the efficiency of electron finders, Internal ZEUS-Note 95-9, DESY (1995)
6. U. Wollmer, Studium der Ortsaufloesung im Hadron-Elektron-Separator des ZEUS-Experimentes, Internal Note DESY F35D-95-09, DESY (1995)
7. F.Goebel, Measurement of the Diffractive Contribution to the DIS Cross Section Using the ZEUS Forward Plug Calorimeter, DESY-Thesis-2001-049, DESY (2001)